



# Application of Deep Convolutional Neural Networks for Analysis of Apparent Density and Porosity of Iron Ore Pellets

Rafael M. Campos<sup>1</sup>, Gustavo M. de Almeida<sup>1</sup>

<sup>1</sup>*Dept. of Control and Automation Engineering, Federal Institute of Espírito Santo - IFES Serra  
Rodovia ES-010 - Km 6,5 - Manguinhos, 29173-087 - Serra - ES, Brasil  
rmofati@gmail.com, gmaia@ifes.edu.br*

**Abstract.** The porosity and apparent density of iron ore pellets directly interfere with the blast furnace process and, therefore, need to be known to assist in its control and optimization. These characteristics are generally calculated using a pycnometer that uses mercury under pressure to fill the pores of the pellet. Considering the need to preserve the environment and the safety of operators, proposals were made to replace this process, but there are several complaints about the repeatability of results achieved, in addition to the time spent in preparing and executing these essays. At the same time, it is possible to observe a remarkable development in Computer Vision and Artificial Intelligence, mainly through Convolutional Neural Networks, which can extract patterns from a set of images and detect these same patterns in images subsequently exposed to this network. In addition to performing classification and detection, the Mask R-CNN network can perform pixel-by-pixel segmentation of objects in images. In its evaluation, the network presented a significantly high mAP and accuracy, demonstrating a satisfactory result for the segmentation and obtaining of porosity and apparent density values, with results similar to the essays currently used.

**Keywords:** Convolutional Neural Networks, Apparent Porosity, Computer Vision, Mask R-CNN, Artificial Intelligence

## 1 Introduction

Technological innovations make industrial processes increasingly agile, fast, efficient, and sustainable. In this context, the conservation of efficiency and sustainability in processes over time becomes crucial for companies.

The creation of ISO 14000, which deals with environmental management and auditing, and its required implementation in Brazilian iron ore mining companies by customers of this product by the main foreign steel companies, is a reflection that environmental management is increasingly important, not only for the important environmental side but also for the economic one as stated by Oliveira et al. [1].

The porosity and apparent density values of iron ore pellets are key factors in the agglomeration and burning processes, belonging to the production stages of iron ore pellets, directly impacting the quality of these pellets. This same importance is analyzed when the pellets are used as raw material in a blast furnace process, directly interfering in it, as quoted by Fonseca [2].

Bayão et al. [3], described in the publication of their study on the influence of porosity on the quality of iron ore pellets, that this characteristic is a parameter that must be well controlled during the process, as this property has a strong influence on the index of reducibility and compressive strength, which are critical factors for the quality of pellets.

Still on the importance of the degree of porosity and its relationship with strength, Bayão et al. [3] claim that the strength of an iron ore pellet decreases with increasing porosity and if this porosity does not meet the criteria of the steel mills, the pellets can break during transport and loading on the blast furnace, reducing its permeability during the process and influencing the quality of the steelworks' final product.

The use of mercury in the process of checking the apparent porosity of an iron ore pellet, using a mercury-filled pycnometer, as described in ISO 15968 and JIS M 8719, does not follow current global needs for the environment, making the handling, reuse, packaging and disposal of pellets that have gone through these tests a

complicated, dangerous and expensive task for companies that practice it in this way, as Y. Omori [4] mentions.

Considering the need to preserve the environment and even due to the development of new technologies, this process was replaced by others that do not use mercury, but other chemical elements and also water, but there are several reports and complaints regarding repeatability of results achieved in these tests using different elements, due to these being able to achieve different pore depths in the pellets as stated by Silva [5].

Ineffective results are also achieved when an operator, with the aid of a caliper, calculates the average diameter of the pellet with ten direct measurements and obtains its weight through a precision scale, reaching through these values and others previously known, the desired apparent density of the iron ore pellet, as also said by Silva [5].

At the same time that we observe the evolution of the tests used to analyze the porosity and apparent density of iron ore pellets, it is possible to observe a remarkable development in the field of Computer Vision and Artificial Intelligence, mainly through Convolutional Neural Networks. Through previous training, these Neural Networks can extract patterns and shapes from a set of training images and subsequently perform the detection of these same patterns, in images exposed to this network, classifying and detecting objects present in them, according to Gonzaga and de Almeida [6].

The R-CNN Neural Mask Network developed by He et al. [7], increments the Faster R-CNN network of Ren et al. [8], developing an object mask in parallel to a bounding box, performing pixel-by-pixel segmentation of objects in images. The created mask fills the pixels of each detected object, creating segregation of it, with the others that are in the same static image or analyzed video frame.

The work proposes to present the use of a previously trained Mask R-CNN network to perform the segmentation of iron ore pellets. Through this segmentation and the weight of each pellet, achieve the porosity and apparent density values, with results similar to the tests described above, bringing more reliability to the processes of iron ore mining companies and their client companies, the steel mills.

This article is divided into five chapters. The first chapter contains a summary of the contextualization of the proposed problem. The second presents the theoretical framework used to support this research. Chapter three describes the methodology used in this research, describing the activities developed and the parameters used for its subsequent reproduction. In the fourth chapter, the results achieved will be presented and in the last chapter, the conclusions of the work will be offered, with the evaluation of the results and proposals for future work.

## 2 Theoretical references

### 2.1 Porosity and bulk density of iron ore pellets

Iron ore is the raw material used in the pig iron production process in a blast furnace. This iron ore is supplied in three different forms to steel companies: in the form of Sinter Feed, which goes through the sintering process and then goes to the blast furnace, the AF Granulate that goes straight to the process, and finally, the Pellet Feed, which goes through the entire pelletizing process, to be fed into the blast furnaces of the steel mills.

During the pelletizing process, the Pellet Feed and other agglomerating materials and mixed additives will go through several stages until reaching the pelletizing disc, in which they will take the form of small spherical pellets, which vary in size according to what is requested by the client steel companies, generally, around 8 to 18mm in diameter Valer [9].

After the pelletizing stage, the formed pellets are sent to the oven to be baked, removing much of the moisture gathered in the previous steps. During pellet cooking, the spaces previously occupied by moisture and air give way to "empty" spaces called pores.

The pores of iron ore pellets are "empty" or gas-filled spaces that may or may not be in contact with the surface of the material. When these spaces are not in contact with the surface, they are called closed pores and when they are, they are called open pores. Open pores are the most harmful to mechanical strength, as many fractures start from superficial defects, as demonstrated by Bayão et al. [3]. Due to the decrease in pellet strength with the increase in the number of pores and its importance for transport processes and even for the blast furnace process, the porosity value of the pellets must be determined. The percentage occupied by pores in the volume of a pellet can be calculated using eq. (1), informed by Silva [5].

$$P = 100 \times \left(1 - \left(\frac{\text{ApparentDensity}}{\text{RealDensity}}\right)\right). \quad (1)$$

As well as the porosity, the Apparent Density of iron ore pellets also directly influences the process of a blast furnace and likewise needs to be checked before being supplied. According to Silva [5], the Apparent Density of an iron ore pellet is governed by eq. (2).

$$\text{ApparentDensity} = \frac{\text{Weight}}{\text{Volume}}. \quad (2)$$

The same author also adds that the Real Density corresponds to the real volume occupied by this pellet, disregarding the value of its porosity. The value of this density is based on the iron content of the batch of minerals and binders that form the pellet.

## 2.2 Convolutional Neural Networks and Their Further Developments

The Convolutional Networks of LeCun et al. [10], also known as Convolutional Neural Networks, or CNN, is a specialized type of Deep Neural Network, for processing data that can be formatted through unidimensional or multidimensional arrays such as images, which can be understood as a grid of pixels in two dimensions. In LeCun et al. [10], a multilayer Artificial Neural Network was developed, called LeNet-5 that could classify handwritten digits from small representations of patterns found in the images presented to the network.

Several developments after the work of LeCun et al. [10] are presented by Gu et al. [11]. The author mentions that since 2006, several methods have been developed to overcome the difficulties encountered in training deep CNN, but he mentions that the AlexNet Krizhevsky and Sutskever [12] network was the one that triggered the first improvements. This network was similar to LeCun et al. [10] LeNet-5 network, but with more layers. Also according to Gu et al. [11], the ResNet network from He et al. [13], that won the ILSVRC 2015 competition is 20 times deeper than the AlexNet network from Krizhevsky and Sutskever [12] and 8 times deeper than the VGGNet developed by Simonyan and Zisserman [14]. The addition of layers to CNNs can improve the approximation of the network activation function to the target with greater non-linearity, achieving better representative characteristics of objects in the images presented to the network.

Girshick et al. [15] proposed a new CNN configuration in order to extract different regions from the same image. This configuration (Fig. 1), was named as Region-based Convolutional Neural Network (R-CNN), as it extracts from the analyzed images, around 2000 regions of interest, instead of trying to classify a huge amount of regions. Subsequently, these regions are analyzed by a CNN and the classification of each one of them will be performed using supervised learning models (SVM). With the new configuration developed, the authors achieved results of 53.3% of mean Average Precision (mAP), a result that was more than 30% higher than the best value obtained by the other competitors of the VOC 2012.

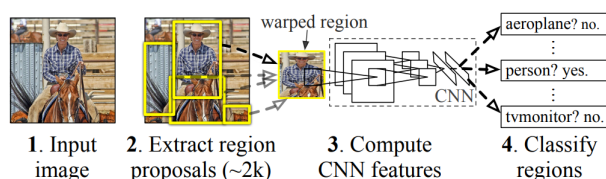


Figure 1. R-CNN model steps. Source: Girshick et al. [15].

The next work from Girshick [16] uses his previously mentioned work and others to obtain greater efficiency in object detection using Deep Convolutional Neural Networks. The previous model has several disadvantages, such as training performed in several stages, training with high processing cost, and high memory usage, in addition to slow object detection. The related disadvantages were solved by replacing the ConvNet that was renewed for each object analyzed by a SPPnet (Spatial Pyramid Pooling networks) that used a model of shared characteristics between the analyzed objects. Concerning his previous work, the new model from Girshick [16] employed several innovations to improve the training and testing speed, in addition to the accuracy in detecting the analyzed objects. This new model (Fig. 2), performed the training of the VGG16 network nine times faster and achieved higher mAP values in the VOC 2012 challenge, than his previous work.

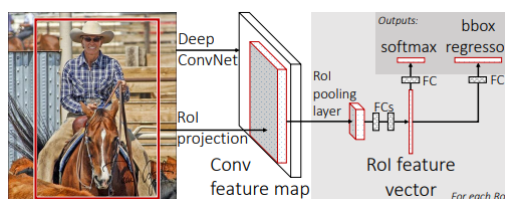


Figure 2. Fast R-CNN model architecture. Source: Girshick [16].

Ren et al. [8] made improvements to the Fast R-CNN model from Girshick [16] in order to achieve real-time object detection, thus developing the Faster R-CNN model. A large part of the reduction in the processing cost was achieved through the sharing of characteristics between the networks used and that was part of the Fast

R-CNN set. This model almost achieved real-time detection, when it ignored the time spent creating the regions that would be analyzed, making this the bottleneck of detection systems. To deal with this bottleneck, the authors developed a network called Region Proposal Network (RPN) which intended to share the convolutional layers with the networks that performed object detection. During the development of the work, the authors observed that the feature maps used by region detectors, such as the Fast R-CNN, could also be used to propose regions. Thus, with the inclusion of convolutional layers, the edges of each region were reduced, achieving a better result in object detection.

Taking advantage of the architecture of the Faster-RCNN model, He et al. [7] developed a new model capable of performing the isolation of objects from images presented to the network through filled pixel to pixel masks. This new model was known as Mask R-CNN and was used to develop this work.

### **2.3 Mask R-CNN**

The method developed by He et al. [7], called Mask R-CNN, increments the Faster R-CNN network from Ren et al. [8] by developing an object mask in parallel with a bounding box. The mask created fills the pixels of the detected object, creating segregation between the others that are in the same static image or analyzed video frame. Although the Faster R-CNN by Ren et al. [8] is not designed to have a pixel-level alignment between the inputs and outputs of the network, a simple and quantization-free layer, called a RoIAlign, which faithfully preserves exact spatial locations. Although simple, this change can directly impact the improvement of mask accuracy with values between 10 to 50%. With all the improvements implemented, the new method outperformed all competitors in the 2016 COCO challenge, reaching rates of 5fps when running on a GPU (200ms per frame of video).

According to He et al. [7], the object detection system in images is formed by four distinct modules. The first of these modules perform the extraction of characteristics of each object in the images. The second is a CNN that creates Regions of Interest based on the outputs of the previous module, that is, through the features that were extracted previously. In the third module, the objects present in each Region of Interest generated in the second module are classified by a CNN. The last module is responsible for performing the segmentation of image objects, through a binary mask applied to each object.

## **3 Methodology**

For the application of deep convolutional neural networks for the apparent density analysis of iron ore pellets, a network based on the Mask R-CNN architecture by He et al. [7] was developed, using the learning transfer technique and fine-tuning from Microsoft COCO dataset weights. The weights from this dataset were used as a starting point for developing our network weights during training, due to their proven robustness and popularity.

No dataset was publicly found for iron ore pellets, so it was necessary to develop a proprietary dataset containing 44 image files of iron ore pellets, presented individually or in groups. The image folder for training the neural network contains 36 images of pellets taken from the internet. The folder used to validate the results, on the other hand, contains 8 images different from those described above, 5 of which belong to the samples that were used for comparison with the results of equipment in use, responsible for carrying out porosity and bulk density tests of a metallurgical laboratory of a mining company. The resolution of images ranges from 259x194 to 4000x2000 pixels. On each folder, an annotation file in JSON format was included, containing information on the positioning and segmentation of the iron ore pellets contained in each image used for training and validation. The annotations were performed using version 2.0.10 of the online tool, VGG Image Annotator (VIA) Dutta et al. [17].

For the development of the neural network algorithm, Google Collaboratory (Colab), an online platform based on the Jupyter Notebook tool, was used. This choice was due to the ease in implementing packages developed by third parties and access to the files of the neural network created, which could be cloned directly from GitHub servers and were hosted on Google Drive. In addition to these facilities, the tool provides limited access to segregated Google server GPUs for this purpose. At the time this work was written, most servers used Nvidia Tesla T4 model GPUs, which mainly allowed less time for training and making the necessary inferences during this development.

For the training of the developed Neural Network, 2000 epochs were performed with the model, which contains 181 instances of pellets in its dataset. Due to the small number of images in the originally created dataset, data augmentation techniques were used to increase the number of samples for network training. The techniques used subsequently allowed an increase in accuracy from 95% to values close to 98%.

The pellet samples (5 units) and the porosity reports containing the results of the tests carried out on each of these were provided by the Vale metallurgical laboratory, located in the city of Vitória/ES, and the results were obtained using the equipment called manual porosimeter, manufactured by ControlVix. Sample data are shown in

Table 1.

Table 1. Sample data provided

Sample	Diameter (pixels)	Diameter (mm)	Volume (cm <sup>3</sup> )	Apparent Density (g/cm <sup>3</sup> )	Porosity (%)
1	2,425	11,28	0,7508	3,2297	35,82
2	2,434	11,31	0,7582	3,2103	36,21
3	2,911	12,08	0,9224	3,1557	37,29
4	2,781	11,80	0,8604	3,2322	35,77
5	3,121	12,23	0,9585	3,2562	35,29

After the detection and segmentation of the pellets present in each image exposed to the network (Fig. 3), diameter measurements were performed in pixels for each pellet. This value was transformed into millimeters, to obtain the actual diameter of the samples.

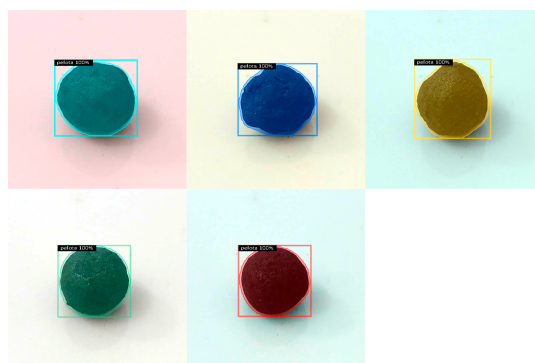


Figure 3. Pellet samples segmented by the Mask R-CNN network.

To obtain the value in millimeters represented by each pixel of the image, the image of a pellet with exactly 12mm in diameter was printed on a blank sheet. This printed image was presented to the network at a distance of 10cm from the camera lens, this being the same distance for obtaining the images of the samples. The image pellet was detected by the net, presenting a mean result of 0.117887mm/pixel.

Thus, this value was used to perform the calculations of apparent density and then porosity, through the formulas previously mentioned, so that it would be possible to directly compare the results with the equipment in use in the laboratories of the mining company in question. The weight values of each sample provided were checked using a precision scale and all these were confirmed.

To verify the results of the model applied to the study, the mean Average Precision (mAP) values will be used, defined by Tan [18], in addition to the accuracy and loss values. These values were automatically calculated by the proposed model during its execution.

## 4 Results

The execution of the 2000 epochs of training the model with the dataset described in the previous topic, were executed in 15.5 minutes on the Google Colab GPUs and the results of accuracy, loss, false positives and false negatives achieved, after the execution of the training, were quite favorable for the developed configuration (Fig. 4).

During the validation of images containing more than one pellet, the algorithm found mainly the pellets that were in the foreground and with their outline completely presented in the images. At first sight, this non-detection may represent an obstacle, but for this work, as we want to present and detect only one pellet in each image presented to the developed network, we will not have this concern.

As seen in the validation image example (Fig. 5), the pellets were segmented correctly and their diameter in pixels was calculated and presented by the network.

With the detection of the pixel diameter results obtained for each of the iron ore pellet samples presented to the network, it was possible to calculate the actual diameter of each pellet in millimeters, then eq. 1 and 2 were

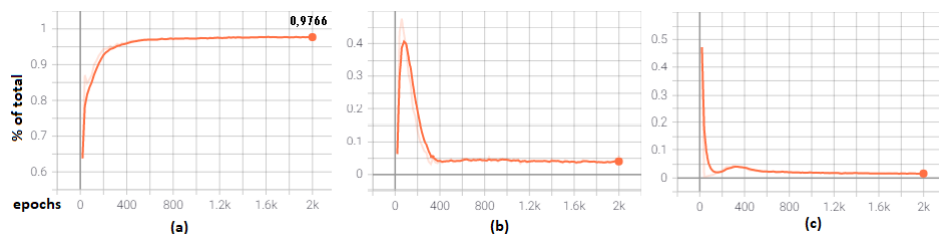


Figure 4. Graphs of (a) accuracy, (b) False Positives and (d) False Negatives of the network.



Figure 5. Image of sample segmented by the Mask R-CNN network, with diameter information in pixels of an iron ore pellet sample.

applied to obtain the percentage of Porosity and Apparent Density of the analyzed samples. The actual density value used to calculate Porosity was informed by the supplier of the samples, corresponding to 5.03226 g/cm<sup>3</sup>. The volume value was calculated using the sphere volume equation. The results achieved were presented in Table 2 and the relative errors in Table 3.

Table 2. Results Achieved Using the R-CNN Mask Network

Sample	Diameter (pixels)	Diameter (mm)	Volume (cm <sup>3</sup> )	Apparent Density (g/cm <sup>3</sup> )	Porosity (%)
1	95.455	11.25	0.7461	3.2503	35.41
2	95.739	11.29	0.7528	3.2334	35.75
3	102.471	12.08	0.9230	3.1539	37.33
4	99.946	11.78	0.8564	3.2472	35.47
5	103.543	12.21	0.9523	3.2774	34.87

Table 3. Relative Errors

Sample	Diameter (mm)	Volume (cm <sup>3</sup> )	Apparent Density (g/cm <sup>3</sup> )	Porosity (%)
1	-0.24%	-0.63%	0.64%	-1.14%
2	-0.21%	-0.71%	0.72%	-1.28%
3	0.00%	0.06%	-0.06%	0.10%
4	-0.15%	-0.46%	0.46%	-0.83%
5	-0.19%	-0.65%	0.65%	-1.18%

## 5 Conclusions

Even with a small number of images, the developed dataset, allowed the Mask R-CNN network model to be trained to detect, segment, and correctly calculate the diameter of iron ore pellets that were exposed to the network,

through static images, present in the dataset of validation. The network met the expectations, segmenting all pellet samples with more than 99% of accuracy during the validation. All relative errors measured were below the 1.3% range (Table 3).

For future work, it is suggested to expand the training and validation dataset, with the use of very different samples in format and size. For this expansion, images with different lighting and presentation should also be used, increasing the number of unique characteristics of the pellets, which could be learned by the model during training.

It is believed that the error presented in the pellet diameter values (Table 3) comes from the difference in methodology as the tests are performed on the equipment in use at the mining company. This equipment performs a simple average of the pellet diameters, through 60 images of each sample, distributed in 6 different positions. For future work, it is suggested that the calculation of the pellet diameter should also be an average of several positions of each sample since the pellets do not have a spherical shape that guarantees the calculation through only one image.

**Acknowledgements.** To the CAPES/FAPES Cooperation - Postgraduate Development Program - PDPG, through the project "TIC+TAC: Information and Communication Technology + Automation and Control Technology, Priority Intelligent Technologies," for the financial support of the research, by through FAPES/CNPq Notice No. 23/2018 - PRONEM (Term of Grant 133/2021 and Process No. 2021-CFT5C).

**Authorship statement.** The authors hereby confirm that they are the sole liable persons responsible for the authorship of this work, and that all material that has been herein included as part of the present paper is either the property (and authorship) of the authors, or has the permission of the owners to be included here.

## References

- [1] D. S. Oliveira, C. V. B. Nunes, de L. Jesus, and A. S. Loiola. *Impactos do Mercúrio no Meio Ambiente e na Saúde*., vol. 5, 2011.
- [2] M. C. Fonseca. *Influência da distribuição granulométrica do pellet feed no processo de aglomeração e na qualidade da pelota de minério de ferro para redução direta*. Dissertação de Mestrado Ouro Preto/MG, 2004.
- [3] D. V. Bayão, R. A. L. Solé, J. J. Mendes, and von F. L. Krüger. e p. S. Assis, "Influência da porosidade na qualidade de pelotas de minério de ferro", in *ABM Proceedings, São Paulo, dez*, pp. 152–164, 2018.
- [4] E. K. Y. Omori. A new method for measuring apparent volume of iron ore pellets in conjunction with determination of the swelling index., *isij int.*, vol. 24, n° 9. pp. 751–753, 1984.
- [5] G. M. Silva. Evolução da automação em ensaios de porosidade em pelotas de minério de ferro. in *ABM Proceedings, São Paulo, out*, pp. 273–281, 2019.
- [6] L. M. Gonzaga and de G. M. Almeida. Artificial intelligence usage for identifying automotive products. *CILAMCE XLI Ibero-Latin-American Congress on Computational Methods in Engineering*, vol. 7, 2020.
- [7] K. He, G. Gkioxari, and P. Dollár. e r. Girshick, "Mask R-CNN", [cs], *jan.*, vol. 2018, 2020.
- [8] S. Ren, K. He, and R. Girshick. e j. Sun, *Faster R-CNN: Towards Real-Time Object Detection with Region Proposal Networks*, [cs], *jan.*, vol. 2016, 2020.
- [9] Valer. *Curso de Mineração - Módulo IV - Pelotização e Uso de Minério de Ferro na Siderurgia*, 2012.
- [10] Y. LeCun, B. Boser, J. S. Denker, D. Henderson, R. E. Howard, W. Hubbard, and L. D. Jackel. Backpropagation applied to handwritten zip code recognition. *Neural Computation*, vol. 1, n. 4, pp. 541–551, 1989.
- [11] J. Gu, Z. Wang, J. Kuen, L. Ma, A. Shahroudy, B. Shuai, T. Liu, X. Wang, L. Wang, G. Wang, J. Cai, and T. Chen. Recent advances in convolutional neural networks, 2017.
- [12] A. Krizhevsky and I. Sutskever. e g. E. Hinton, *ImageNet classification with deep convolutional neural networks*, *Commun. ACM*, vol. 60, pp. 84–90, 2017.
- [13] K. He, X. Zhang, and S. Ren. e j. In D. Residual, ed, *Sun*, pp. 770–778, in 2016 IEEE Conference on Computer Vision and Pattern Recognition (CVPR), Las Vegas, NV, USA, jun p. Learning for Image Recognition, 2016.
- [14] K. Simonyan and A. Zisserman. Very deep convolutional networks for large-scale image recognition. *arXiv preprint arXiv:1409.1556*, 2014.
- [15] R. Girshick, J. Donahue, and T. Darrell. e j. Malik, *Rich feature hierarchies for accurate object detection and semantic segmentation*, [cs], *out*, vol. 2014, 2020.
- [16] R. Girshick. Fast r-cnn. In *Proceedings of the IEEE international conference on computer vision*, pp. 1440–1448, 2015.
- [17] A. Dutta, A. Gupta, and A. Zisserman. *VGG Image Annotator (VIA)*. University of, Oxford, 2018.
- [18] R. J. Tan. *Breaking down Mean Average Precision (mAP)*. Graduation conclusion work, NUS MTech, 2019.